

CalibQuant: 1-Bit KV Cache Quantization for Multimodal LLMs

*Insu Han¹, *Zeliang Zhang², *Zhiyuan Wang³, *Yifan Zhu²,
 Susan Liang², Jiani Liu², Haiting Lin⁴, Mingjie Zhao⁵, Chenliang Xu², †Kun Wan⁴, †Wentian Zhao⁴
¹KAIST ²University of Rochester ³UCSB ⁴Adobe Inc. ⁵Independent Researcher
 insu.han@kaist.ac.kr,
 {zeliang.zhang, yifan.zhu, susan.liang, chenliang.xu}@rochester.edu,
 jliu186@u.rochester.edu, {wezhao, kuwan, halin}@adobe.com
 zwang796@ucsb.edu, mjzhaol@gmail.com

Abstract

*Multimodal Large Language Models (MLLMs) have demonstrated remarkable performance across diverse applications. However, their computational overhead during deployment remains a critical bottleneck. While Key-Value (KV) caching effectively trades memory for computation to enhance inference efficiency, the growing memory footprint from extensive KV caches significantly reduces throughput and restricts prolonged deployment on memory-constrained GPU devices. To address this challenge, we propose CalibQuant, a simple yet highly effective visual quantization strategy that drastically reduces both memory and computational overhead. Specifically, CalibQuant introduces an extreme 1-bit quantization scheme, complemented by novel post-scaling and calibration techniques tailored to the intrinsic patterns of KV caches, thereby ensuring high efficiency without compromising model performance. Leveraging Triton for runtime optimization, we achieve a **10x** throughput increase on InternVL models. Our method is designed to be plug-and-play, seamlessly integrating with various existing MLLMs without requiring architectural changes. Extensive experiments confirm that our approach significantly reduces memory usage while maintaining computational efficiency and preserving multimodal capabilities. Codes are available at <https://github.com/insuhan/calibquant>.*

1. Introduction

Multimodal Large Language Models (MLLMs) have demonstrated strong performance across a wide range of tasks including automated caption generation, interactive storytelling, medical image diagnostics and emotion-driven cap-

tioning, to name a few [3, 5, 24]. However, due to the quadratic computation complexity and linear memory complexity of the self-attention mechanism [2], Transformer-based MLLMs present significant challenges in terms of memory consumption as the number of visual frames and the image resolution increase [36]. The resulting surge in visual tokens further amplifies the computational burden, making the deployment of MLLMs in real-world applications increasingly difficult. To address these challenges and accelerate MLLMs, various approaches have been proposed to reduce computational costs and improve throughput. These include developing compact multimodal language models [1], applying model pruning [35, 36], leveraging mixture-of-experts strategies [10, 15], and optimizing KV cache mechanisms [12, 13, 28, 32–34].

Among these acceleration methods, KV cache optimization has gained widespread popularity due to its scalability across different models. By storing and reusing intermediate key and value (KV) states during decoding, it allows us to avoid operations running in quadratic time in the number of tokens. The KV cache trades memory for computational efficiency. However, as the size of the KV cache increases linearly in the number of generated tokens, it causes a memory bottleneck.

In this work, we study an approach to quantize the KV cache in MLLMs, i.e., retaining all token embeddings while storing them in a low-bit format. We begin with the well-known uniform integer quantization technique [29], widely adopted for its simplicity. However, when applied to MLLMs, global uniform quantization across the KV cache fails to capture the distinct distributional properties of visual tokens, leading to significant quantization errors, especially at extremely low-bit levels. To address this, we apply channel-wise quantization for the key cache. This approach has been previously observed in [20] for LLMs, where a small subset of channels in key cache contains outliers, making channel-wise quantization particularly effective. How-

* indicates the equal contribution with random order.

† indicates the project leaders.

ever, to the best of our knowledge, this is the first observation of its superiority in MLLMs, particularly for handling visual tokens, where distributional variations are more pronounced. Additionally, we propose a post-scaling trick that leverages the linearity of the dequantization process to restore the key cache from low-bit precision to full precision. We defer these operations but apply a similar transformation to the query state. Since the query represents only a single token during decoding, this approach significantly improves computational efficiency.

We further observe that outliers in the KV cache can distort the attention mechanism, as extreme values are over-represented post-quantization, degrading performance. To mitigate this, we introduce a novel post-quantization calibration strategy that adjusts pre-softmax attention scores by aligning their distributions with unquantized baselines, effectively reducing the impact of extreme value distortions. Our experiments show that after applying this calibration, the distribution of pre-softmax attention scores closely matches the unquantized baseline, yielding performance nearly identical to full-precision models. These contributions collectively enable efficient, low-bit KV cache quantization tailored for MLLMs, preserving multimodal reasoning capabilities while significantly reducing memory overhead.

Our contributions can be summarized as follows:

- We introduce a novel 1-bit quantization for the visual KV cache in MLLMs, demonstrating superior performance across diverse tasks such as image captioning (COCO Caption), video understanding (MMBench-Video), and document visual question answering (DocVQA).
- Our method builds on uniform integer quantization applying channel-wise scheme for both key and value caches. Additionally, we propose a post-quantization calibration technique to adjust pre-softmax attention scores, effectively reducing the impact of extreme values and improving not only approximation quality but also the end-to-end performance.
- We implement our quantization algorithm using the Triton kernel, achieving significant acceleration in the decoding stage with a speedup of up to $11.24\times$ compared to the 16-bit baseline. In particular, we introduce a post-scaling trick further optimizes computational efficiency by deferring dequantization, reducing memory overhead.

2. Related Work

Efficient Inference of MLLMs. Multimodal large language models (MLLMs) typically contain billions of parameters, posing significant challenges in both memory consumption and computational efficiency during deployment. Numerous studies have explored cost reduction strategies for MLLM deployment, including designing compact multimodal models [1, 8, 9, 18, 19, 31], model pruning [6, 23, 30, 36], and hardware-software co-optimization [17]. However,

the self-attention mechanism, which has quadratic computational complexity, remains a bottleneck [27]. As input sequence length increases, both memory usage and computational burden grow correspondingly. During decoding, every generated token involves computations over all preceding input tokens, exacerbating inefficiencies.

KV Cache Compression. The KV cache technique has been introduced to mitigate redundant computations [34]. By caching key and value embeddings in memory, the KV cache allows the model to reuse stored information instead of recomputing attention scores for all previous tokens. This approach effectively trades off memory usage for computational efficiency, significantly improving inference speed. While the KV cache technique substantially reduces computational overhead, it introduces a new bottleneck: memory consumption. This issue becomes increasingly critical in scenarios involving long-context generation and multi-turn conversations, where growing input lengths negatively impact throughput.

A common approach to reducing the size of the KV cache is to remove or evict unimportant key and value vectors from the cache. A line of research explores various importance scores to evict tokens [4, 16, 34]. Quantization techniques provide another path to reducing KV cache memory overhead by transforming floating-point representations into lower-precision integers, thus significantly reducing memory usage and potentially enhancing inference speed. Methods such as KIVI [20] have introduced asymmetric quantization strategies. KVQuant [14] introduces advanced KV cache quantization techniques, including per-channel, pre-RoPE, non-uniform, and per-vector quantization, significantly improving accuracy at low bitwidths. QJL [32] leverages a Johnson-Lindenstrauss (JL) transform combined with sign-bit quantization to eliminate the storage overhead associated with quantization constants in KV cache quantization. In contrast to these approaches developed primarily for general-purpose LLMs, our method specifically addresses the unique challenges of MLLMs, where visual tokens dominate the KV cache and present distinct statistical patterns. By carefully exploiting the distributional characteristics of visual activations, we introduce a specialized channel-wise quantization combined with attention-aware calibration, significantly reducing memory footprint while preserving multimodal reasoning capabilities.

3. Preliminaries

3.1. KV Cache for Efficient Token Generation

In autoregressive sequence generation with Transformers [27], the key-value (KV) cache improves efficiency by eliminating redundant computation in self-attention. The token generation process consists of two stages: **prefill** and

decoding.

In the **prefill** stage, the model processes a prompt of length n and computes key and value for all tokens in a form of matrices $K \in \mathbb{R}^{n \times d}, V \in \mathbb{R}^{n \times d}$ where d is the embedding dimension. These caches store past key and value embeddings, enabling efficient self-attention without recomputation in the next token generation steps.

In the **decoding** stage, the model generates one token at a time. Given a query vector $q_{\text{new}} \in \mathbb{R}^{1 \times d}$ and its corresponding key-value pair $(k_{\text{new}}, v_{\text{new}})$, the KV cache updates by appending the new key and value:

$$K \leftarrow [K; k_{\text{new}}], \quad V \leftarrow [V; v_{\text{new}}]. \quad (1)$$

The attention output is then computed as:

$$\text{softmax} \left(\frac{q_{\text{new}} K^T}{\sqrt{d}} \right) V. \quad (2)$$

This incremental update reduces the time complexity of self-attention from $O(n^2 d)$ to $O(nd)$ per step. While this explanation considers a single layer and head, the same mechanism applies across multiple layers and heads in practical Transformer models.

3.2. Uniform Integer Quantization

Quantization is a process that reduces high-precision floating-point values (e.g., 32-bit floating point) to lower-precision integer representations (e.g., 8-bit integer). This compression not only reduces memory space but also accelerates computation speed, which is particularly useful in resource-constrained environments like edge devices and accelerators.

A widely used approach is the uniform integer quantization. Given a bitwidth $b > 0$ and an input value x within a range $[\alpha, \beta]$ for some $\beta > \alpha$, it is mapped to a discrete integer $x_{\text{dis}} \in \{0, 1, \dots, 2^b - 1\}$ computed as

$$x_{\text{dis}} = \left\lfloor (x - \alpha) \cdot \frac{2^b - 1}{\beta - \alpha} \right\rfloor, \quad (3)$$

where $\lfloor \cdot \rfloor$ denotes the rounding operator. Representing x_{dis} requires b bits and it can reduce memory requirements significantly when b is smaller than the full precision.

To recover an approximate floating-point representation, the dequantization process converts it back as follows:

$$x_{\text{deq}} = x_{\text{dis}} \cdot \frac{\beta - \alpha}{2^b - 1} + \alpha. \quad (4)$$

This can be naturally extended to vectors or matrices by applying entry-wise.

4. CalibQuant: Low-Bit Quantization of Visual KV Cache via Calibration

Tokens in multimodal large language models (MLLMs) encompass multiple modalities. For instance, vision-language

models like InternVL process both textual and visual tokens. In this work, we focus on scenarios where visual tokens dominate, meaning their sequence length exceeds that of textual tokens such as image captioning and video understanding tasks involving text. In these cases, the KV cache for visual tokens becomes a memory bottleneck. To improve the efficiency of token generation, we propose applying the uniform integer quantization to the visual KV cache.

Given a KV cache, we first determine appropriate values α and β that serve as the lower and upper bounds for all entries in the cache. The cache is then encoded into b -bit representations, where the bitwidth b controls the trade-off between memory efficiency and attention accuracy; smaller b values lead to greater information loss. Our primary objective is to quantize visual KV caches to low-bit precision, such as $b = 2$ or 1 , while minimizing performance degradation. To improve the accuracy of low-bit quantization in the visual cache, we incorporate two simple yet effective strategies: channel-wise quantization and calibration.

4.1. Channel-wise Quantization with Post-scaling

In order to apply the quantization in Eq. (3), one needs to determine the minimum and maximum values of the target vectors, i.e., α and β . While a naïve approach would compute these extreme values using global statistics, we instead refine the statistical range along the channel axis. Specifically, let $K \in \mathbb{R}^{n \times d}$ be a key cache where n and d denote the number of tokens and the head dimension, respectively. We define vectors $\alpha, \beta \in \mathbb{R}^d$ as:

$$\alpha_i = \min_{j \in [n]} K_{j,i}, \quad \beta_i = \max_{j \in [n]} K_{j,i} \quad (5)$$

for each $i \in [d]$. Each row vector in K is then quantized using Eq. (3) and (4), where the multiplication is applied entry-wise. We similarly implement this channel-wise uniform quantization approach for the value cache.

Channel-wise quantization was previously studied by Liu et al. [20] and introduced as KIVI. However, their approach applied channel-wise quantization to the key cache and a token-wise method to the value cache in language models. In contrast, for MLLMs, we find that applying channel-wise quantization to both the key and value caches yields superior performance compared to KIVI. Additionally, we verify that global quantization of the value cache degrades performance compared to our approach. See Sec. 5 for details.

Post-scale for Efficiency Key Cache Management. The quantized key cache can be represented by discretized integer values, a scale factor and a bias term. During the decoding stage, these components are utilized to dequantize and reconstruct the key cache, which is subsequently multiplied by the query. However, channel-wise quantization requires distinct scale and bias vectors, resulting in numerous unique

values and increased computational overhead during dequantization. In addition, this makes computations in the CUDA kernel inefficient. By observing that the quantized keys have a limited set of discrete values (e.g., 0,1,2,3 for 2-bit quantization), we leverage a simple algebraic rearrangement to reduce storage and improve computational efficiency.

More formally, let $k \in \mathbb{R}^d$ be any row vector within the key cache $K \in \mathbb{R}^{n \times d}$ and k_{dis} be its b -bit integer quantization, accompanied by channel-wise scaling factors $\alpha, \beta \in \mathbb{R}^d$. Given a query $q \in \mathbb{R}^d$, the attention in token generation requires the computation of:

$$\begin{aligned} q \cdot k_{\text{deq}} &= q \cdot \left(k_{\text{dis}} \odot \frac{\beta - \alpha}{2^b - 1} + \alpha \right) \\ &= \left(q \odot \frac{\beta - \alpha}{2^b - 1} \right) \cdot k_{\text{dis}} + q \cdot \alpha \end{aligned} \quad (6)$$

where \cdot and \odot denote the inner-product and entry-wise product between vectors, respectively. In particular, the channel-wise dequantization operation $\left(k_{\text{dis}} \odot \frac{\beta - \alpha}{2^b - 1} + \alpha \right)$ is deferred and efficiently integrated into the subsequent vector multiplications. Furthermore, this approach stores only the b -bit integer quantized values, avoiding full-precision dequantization computations whose dimension scales with token length n , thereby substantially reducing memory requirements. Consequently, this approach ensures the efficiency of low-bit uniform quantization with channel-wise scaling. The post-scale approach can be naturally applied to the dequantization of the value cache.

4.2. Calibration of Post-quantization

A crucial drawback of uniform quantization, as discussed in Sec. 3.2, is that the dequantized values tend to contain a larger number of extreme values. This arises because the quantization codebook always includes the minimum and maximum values, causing inputs that are closest to these bounds to be mapped to these extremes upon dequantization. For example, when $b = 1$ (1-bit quantization), each element in the dequantized vector x_{deq} is restricted to be either α or β . Consequently, the reconstructed KV cache often contains disproportionately large absolute values, resulting in distorting the output of attentions.

To address this issue, we propose a novel post-quantization calibration that adjusts the peak values of pre-softmax attention scores. More precisely, consider a query vector $q \in \mathbb{R}^d$ and a key cache $K \in \mathbb{R}^{n \times d}$, with K_{deq} denoting the dequantized key cache. Let K_{deq} be the dequantization of K . The pre-softmax attention scores are computed as $qK_{\text{deq}}^T/\sqrt{d}$. We investigate empirical distributions of the elements in both qK^T/\sqrt{d} and $qK_{\text{deq}}^T/\sqrt{d}$, using InternVL2.5-8B model on COCO Caption dataset [7], applying 1-bit quantization to the visual key cache. Fig. 1 illustrates normalized histograms of the pre-softmax attention

scores for a randomly selected head and layer, comparing the exact scores (Exact) with those obtained from simple quantization (Quant, blue). The results show that naive quantization significantly disturbs the distribution shape and introduces excessive outliers in $qK_{\text{deq}}^T/\sqrt{d}$. This justifies the need for an additional correction.

Motivated by these findings, we introduce a post-quantization calibration by re-scaling the pre-softmax attention scores. Specifically, suppose that all elements in $qK_{\text{deq}}^T/\sqrt{d}$ are in the interval $[\gamma, \delta]$. Given $\tau_1, \tau_2 > 0$, we define a linear transformation g mapping from $[\gamma, \delta]$ to $[\gamma - \tau_1, \delta - \tau_2]$ for $\tau_1, \tau_2 > 0$, given by:

$$g(x) := \frac{\delta - \gamma + \tau_1 - \tau_2}{\delta - \gamma} (x - \gamma) + \gamma - \tau_1. \quad (7)$$

The attention scores are then adjusted as follows:

$$\text{softmax} \left(g \left(\frac{qK_{\text{deq}}^T}{\sqrt{d_k}} \right) \right). \quad (8)$$

We search for the best calibration parameters τ_2, τ_1 using a grid search among $\tau_1, \tau_2 \in \{0, 1, 2, 3\}$ and fix it across all prompt inputs, layers, and attention heads. As in Fig. 1, the calibration (Quant-C, red) effectively mitigates the impact of extreme values, aligning the distribution of the adjusted scores more closely with that of the exact baseline (Exact) compared to the uncalibrated quantization (Quant, blue). Furthermore, as illustrated in Fig. 2, the proposed calibration reduces the mean squared error (MSE) in approximating the attention scores across all layers, outperforming quantization-only approach. Experimental result in Sec. 5.5 confirms that this calibration significantly enhances performance on our benchmarks, achieving substantial improvements over the baseline.

4.3. Implementation Details

To develop a practical implementation, we consider multi-head attention with h heads. For example, a query can be represented as $q \in \mathbb{R}^{h \times 1 \times d}$. Note that attention computation with quantization requires two key operations: (1) qK_{dis}^T and (2) wV_{dis} where $K_{\text{dis}}, V_{\text{dis}} \in \{0, 1, \dots, 2^b - 1\}^{h \times n \times d}$ are discretized KV caches with bitwidth b and $w \in \mathbb{R}^{h \times 1 \times n}$ is the attention scores defined in Eq. (8).¹ Although these multiplications are conceptually straightforward, several obstacles must be addressed to enable an efficient implementation:

- Lack of hardware intrinsics: While modern GPUs support microscaling formats [22] to accelerate quantized models down to 4-bit floating points, hardware intrinsics for lower-precision (e.g., 1-bit) encoding remain unavailable.

¹The matrix multiplications are performed independently along the first axis, enabling parallel computation.

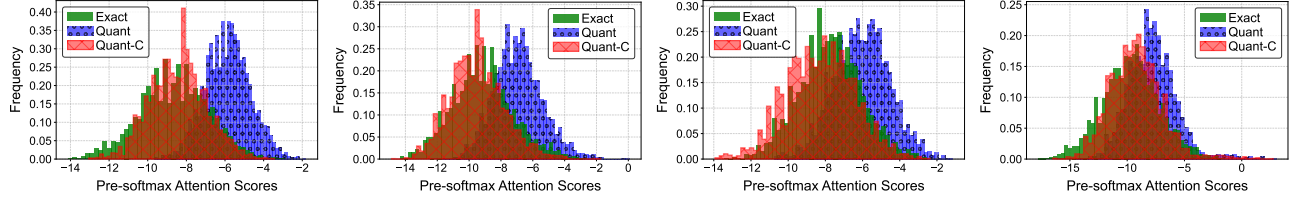


Figure 1. Distribution of entries in qK^T/\sqrt{d} without quantization (Exact, green), with quantization (Quant, blue) and calibration on post-quantization (Quant-C, red) across different layers and heads.

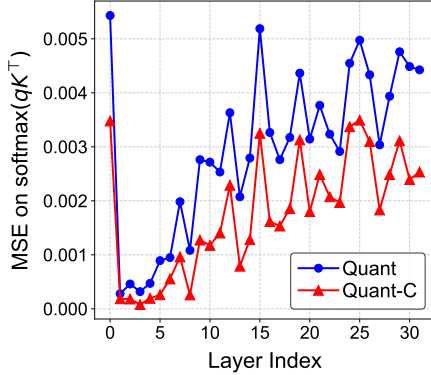


Figure 2. Mean squared error (MSE) for $\text{softmax}(qK^T/\sqrt{d})$ across multiple layers. The quantization with calibration (Quant-C, red) shows much lower errors than the quantization only method (Quant, blue).

- Overhead in matrix multiplication: A naive approach with separate operations fails to reduce host-to-GPU data transfer volumes while introducing additional computational overhead compared to standard matrix multiplication.
- Irregular matrix shape: Quantization is only partially applied to the visual cache, resulting in computations involving irregular matrix dimensions.

To overcome these challenges, we pack the quantized values into the smallest bitwidth (e.g., 8-bit from PyTorch) supported by the GPU. This packing process involves shifting and summing the quantized values to form compact integer representations. More details on packing indices are provided in Appendix A.1. Additionally, we leverage Triton [25] to generate optimized kernels that fuse unpacking (decoding) directly into matrix multiplication operations. For qK_{dis}^T , the reduction dimension (i.e., d) corresponds to compressed input data, which remains compact after unpacking. This compactness enables processing multiple matrices concurrently within each streaming multiprocessor (SM). By doing so, a larger tile of q can be retained in shared memory throughout the computation, reducing costly global memory accesses and improving throughput, as shown in Algorithm 1. For wV_{dis} , the reduction dimension (i.e., n) can be large (for long-context input or visual tokens), while the output dimen-

sion remains short. This asymmetry allows the kernel to retain a single stripe of w in shared memory throughout the computation, minimizing memory traffic. This constraint favors fine-grained task division across streaming multiprocessors (SMs), where smaller, independent workloads are distributed dynamically to maximize occupancy and hide memory latency. Algorithm 2 demonstrates the workload distribution in the wV_{dis} kernel.

Algorithm 1: qK_{dis}^T Kernel with Fused Unpacking

Input : $q \in \mathbb{R}^{h \times 1 \times d}$, $K_{\text{dis}} \in \{0, \dots, 2^b - 1\}^{h \times n \times d_{\text{pack}}}$,
block sizes b_h, b_n

Output : pre-softmax attention scores

Procedure qk_kernel

```

pid ← program_id ;
start ←  $b_h \times \text{pid}$  ;
end ←  $(b_h + 1) \times \text{pid}$  ;
 $q \leftarrow Q[\text{start} : \text{end}, :, :]$  ; // stays in shared
memory
for  $j \leftarrow 0$  to  $n$  step  $b_n$  do
     $k \leftarrow K_{\text{dis}}[\text{start} : \text{end}, j : j + b_n, :]$  ;
     $k' \leftarrow \text{load}(\text{unpack}(k))$  ;
     $u \leftarrow q \odot k'$  ; // Element-wise
    multiplication with boardcast
     $v \leftarrow \sum u$  along axis=1 ;
    store(v)

```

5. Experiment

We evaluate the proposed quantization method across multiple tasks where MLLMs demonstrate strong performance. First, we benchmark image captioning task on the COCO Caption dataset [7]. Next, we conduct document visual question answering on the DocVQA dataset [21]. We then evaluate video understanding performance on the MMBench-Video [11]. Finally, we report inference speed of our method by measuring throughput. All experiments were performed using NVIDIA H100 GPUs with 80GB VRAM.

5.1. Image Captioning

We test our quantization method on the image captioning task using the COCO Caption dataset [7]. We use the fol-

Algorithm 2: wV_{dis} Kernel with Fine-Grained Task Division

Input : $w \in \mathbb{R}^{h \times 1 \times n}$, $V_{\text{dis}} \in \{0, \dots, 2^b - 1\}^{h \times n \times d_{\text{pack}}}$,
number of all physical SMs P , block size b_h

Output : attention output with quantized cache

Procedure wv_kernel

```
pid  $\leftarrow$  program_id ;
 $x \leftarrow \frac{d_{\text{pack}}}{b_h}$  ;           // Blocks per matrix
 $y \leftarrow \lceil \frac{h \times x}{P} \rceil$  ;       // Tasks per SM
 $s \leftarrow y \times \text{pid}$  ;
 $t \leftarrow y \times (\text{pid} + 1)$  ;
 $i \leftarrow s$  ;
while  $i \neq t$  do
   $\text{matrix} \leftarrow \lfloor \frac{i}{x} \rfloor$  ;       // Matrix index
   $\text{end} \leftarrow \min((\text{matrix} + 1) \times b_h, t)$  ;
   $w \leftarrow w[\text{matrix}, :, :]$  ;     // Load  $w$  stripe
  into shared memory
  for  $j \leftarrow i$  to  $\text{end}$  do
     $\lfloor$  compute output[ $\text{matrix}, :, j \times b_h : (j+1) \times b_h$ ]
   $i \leftarrow \text{end}$  ;
```

lowing models: llava-1.5-7b, 13b, and internvl-2.5-8b, 26b. An input prompt is constructed with a system prompt and the image tokens and evaluates the output generation using standard captioning metrics, including BLEU, METEOR, ROUGE-L, SPICE, and CIDEr, to assess both lexical similarity and semantic coherence with ground-truth captions. We compare our quantization with other KV cache quantization or compression methods including KIVI [20] and VLCache [26]. For VLCache, we adjust its hyperparameter such as compression ratio so that the total memory budget matches that in others. For each model, we evaluate the quality of generations where the bitwidth b of each method is changing from 8 to 1.

Tab. 1 summarizes the results. The proposed method (“Ours”) consistently demonstrate competitive or superior performance across different bitwidths (8, 4, 2, and 1 bits) compared to the baseline (16-bit) and other methods such as VLCache and KIVI. In particular, for llava-1.5-7b, our method achieves the highest CIDEr score of 1.105 at 8 bits, matching the baseline, and improved to 1.109 at 1 bit, surpassing VLCache (1.053). Similarly, for internvl-2.5-26b, our method yielded the highest CIDEr score of 1.32 at 4 bits and 1.313 at 2 bits, outperforming both VLCache and KIVI. These results highlight the efficacy of our approach in maintaining or enhancing performance under reduced bitwidths, demonstrating its robustness across diverse model architectures and quantization levels.

5.2. Document Visual Question Answering

Next, we evaluate the performance of our method on document visual question answering task using the DocVQA

dataset [21] with the internvl-2.5 models. Performance is evaluated using the Average Normalized Levenshtein Similarity (ANLS), where higher values indicate better accuracy. Our proposed method demonstrates robust performance across different bitwidths (4, 2, and 1 bits) compared to the baseline (16-bit) and other competing methods including KIVI and VLCache. Results are reported in Tab. 2. Observe that at 4 bits our method achieves ANLS scores of 0.9138 and 0.9237 for each model respectively, closely matching or slightly exceeding the baseline scores of 0.9135 and 0.9242. At 2 bits, our method maintains competitive performance with ANLS values of 0.8937 and 0.9037, outperforming KIVI (0.8877 and 0.9056) and VLCache (0.8881 and 0.8869). Even at the challenging 1-bit level, our method achieves ANLS scores of 0.8455 and 0.8894, surpassing KIVI (0.8023 and 0.8617) and performing comparably to VLCache (0.8558 and 0.87). These results highlight the efficacy of our approach in preserving accuracy under aggressive quantization, demonstrating its versatility and adaptability across different model sizes on the DocVQA task.

5.3. Video Understanding

We benchmark quantization methods on the video understanding task using the MMBench-Video dataset [11]. Table 3 presents the results of different quantization techniques applied to the internvl-2.5 models, evaluating both perception and overall scores. The baseline with 16-bit full-precision achieves the highest scores, serving as an upper bound for comparison.

Our method consistently outperforms both KIVI and VLCache across all bitwidths. In particular, at 8-bit and 4-bit, it nearly matches the full-precision baseline, demonstrating minimal loss in perception and overall scores. Even at 2-bit, our approach surpasses VLCache and KIVI, preserving better performance. At 1-bit, while performance naturally degrades, our method still outperforms VLCache and KIVI in overall score (0.8894 vs. 0.87 and 0.8617), suggesting improved resilience at extreme quantization.

At 8 bits, our method achieves perception and overall scores of 1.53 and 1.5 for internvl-2.5-8b model, matching the baseline, and 1.68 for both metrics in 26b model, also aligning with the baseline. At 4 bits, our method outperforms others with scores of 1.54 and 1.51 for 8b model, and 1.69 and 1.68 for 26b model, surpassing VLCache (1.53 and 1.5; 1.68 and 1.67) and KIVI (1.5 and 1.47; 1.66 and 1.65). At 2 bits, our method maintained strong performance, particularly for 26b model, with scores of 1.67 and 1.66, compared to VLCache (1.64 and 1.64) and KIVI (1.64 and 1.63). However, at 1 bit, our method slightly underperforms the VLCache with marginal degradations.

Methods	Bitwidth b	Evaluation Metrics (\uparrow)							
		SPICE	BLEU_1	BLEU_2	BLEU_3	BLEU_4	METEOR	ROUGE_L	CIDEr
Model: llava-1.5-7b									
Baseline	16	0.235	0.731	0.563	0.413	0.295	0.292	0.558	1.105
VLCache	8	0.233	0.732	0.563	0.413	0.295	0.291	0.556	1.103
Ours	8	0.235	0.731	0.563	0.413	0.295	0.293	0.558	1.105
KIVI	4	0.235	0.730	0.563	0.413	0.296	0.293	0.558	1.106
VLCache	4	0.230	0.731	0.560	0.410	0.293	0.288	0.554	1.091
Ours	4	0.235	0.730	0.563	0.413	0.296	0.293	0.558	1.105
KIVI	2	0.235	0.728	0.560	0.410	0.293	0.292	0.556	1.099
VLCache	2	0.225	0.729	0.557	0.406	0.289	0.285	0.550	1.074
Ours	2	0.235	0.729	0.561	0.412	0.295	0.292	0.557	1.099
VLCache	1	0.218	0.723	0.551	0.401	0.284	0.281	0.545	1.053
Ours	1	0.227	0.739	0.571	0.419	0.300	0.287	0.558	1.109
Model: llava-1.5-13b									
Baseline	16	0.239	0.747	0.582	0.434	0.316	0.296	0.564	1.159
VLCache	8	0.236	0.752	0.585	0.436	0.316	0.294	0.565	1.163
Ours	8	0.239	0.747	0.582	0.434	0.316	0.296	0.565	1.159
KIVI	4	0.240	0.747	0.583	0.435	0.316	0.296	0.565	1.160
VLCache	4	0.233	0.752	0.586	0.436	0.317	0.292	0.563	1.166
Ours	4	0.239	0.747	0.582	0.434	0.316	0.296	0.564	1.159
KIVI	2	0.240	0.742	0.578	0.430	0.313	0.296	0.563	1.149
VLCache	2	0.227	0.753	0.586	0.436	0.316	0.288	0.559	1.150
Ours	2	0.239	0.746	0.581	0.433	0.314	0.295	0.564	1.155
VLCache	1	0.223	0.751	0.584	0.434	0.314	0.284	0.556	1.137
Ours	1	0.230	0.764	0.597	0.445	0.323	0.288	0.566	1.168
Model: internv1-2.5-8b									
Baseline	16	0.235	0.795	0.629	0.477	0.352	0.292	0.580	1.257
VLCache	8	0.236	0.794	0.628	0.476	0.351	0.291	0.580	1.252
Ours	8	0.236	0.795	0.630	0.476	0.351	0.292	0.580	1.257
KIVI	4	0.232	0.8	0.635	0.481	0.355	0.289	0.580	1.255
VLCache	4	0.237	0.793	0.628	0.475	0.350	0.291	0.579	1.252
Ours	4	0.236	0.795	0.630	0.477	0.352	0.292	0.580	1.259
KIVI	2	0.233	0.801	0.635	0.480	0.354	0.290	0.581	1.252
VLCache	2	0.235	0.793	0.628	0.474	0.349	0.290	0.577	1.250
Ours	2	0.232	0.798	0.632	0.477	0.351	0.289	0.579	1.254
KIVI	1	0.230	0.784	0.617	0.464	0.339	0.285	0.572	1.194
VLCache	1	0.232	0.792	0.625	0.472	0.347	0.288	0.574	1.236
Ours	1	0.231	0.792	0.625	0.471	0.346	0.287	0.577	1.231
Model: internv1-2.5-26b									
Baseline	16	0.244	0.813	0.653	0.499	0.374	0.300	0.594	1.321
VLCache	8	0.242	0.813	0.654	0.501	0.375	0.299	0.593	1.321
Ours	8	0.244	0.813	0.654	0.499	0.374	0.300	0.593	1.321
KIVI	4	0.239	0.808	0.644	0.489	0.361	0.296	0.588	1.289
VLCache	4	0.241	0.813	0.653	0.501	0.375	0.298	0.591	1.319
Ours	4	0.243	0.813	0.654	0.500	0.374	0.300	0.594	1.320
KIVI	2	0.239	0.806	0.643	0.488	0.362	0.296	0.588	1.284
VLCache	2	0.238	0.809	0.648	0.495	0.371	0.295	0.587	1.302
Ours	2	0.243	0.812	0.651	0.497	0.371	0.299	0.592	1.313
KIVI	1	0.237	0.794	0.631	0.479	0.355	0.292	0.579	1.261
VLCache	1	0.234	0.802	0.640	0.488	0.364	0.291	0.582	1.282
Ours	1	0.238	0.802	0.640	0.486	0.360	0.293	0.586	1.280

Table 1. Performance evaluations on COCO Caption [7] of various KV cache compression methods for different models. Among all metrics, the CIDEr score is the most conclusive metric for image captioning, aligning closely with human judgment.

5.4. Runtime Analysis

To show the impact of our quantization on decoding efficiency, we evaluated the throughput (i.e., the number of generated tokens per second) of the proposed 1-bit quantization method against a 16-bit baseline using the internv1-2.5 models. We consider two scenarios where the lengths of

the visual tokens are $n = 3328$ and 8192 . We vary the maximum GPU memory from 5 GB to 30 GB and for each memory constraint we find the maximum number of batch size to fit in and measure throughput of the decoding stage. Fig. 3 demonstrates that our 1-bit quantization method consistently outperforms the baseline in all memory budgets.

Methods	Bitwidth b	ANLS (\uparrow)			
		internvl-2.5		llava-1.5	
		8b	26b	7b	13b
Baseline	16	0.9135	0.9242	0.2131	0.2368
KIVI	8	0.9072	0.9072	-	-
VLCache	8	0.9121	0.9212	0.2055	0.2278
Ours	8	0.9131	0.9241	0.2131	0.2368
KIVI	4	0.9074	0.9074	0.2127	0.2367
VLCache	4	0.9048	0.9091	0.1955	0.2196
Ours	4	0.9138	0.9237	0.2133	0.2368
KIVI	2	0.8877	0.9056	0.2116	0.2379
VLCache	2	0.8881	0.8869	0.1865	0.2089
Ours	2	0.8937	0.9037	0.2133	0.2368
KIVI	1	0.8023	0.8617	-	-
VLCache	1	0.8558	0.8700	0.1783	0.1960
Ours	1	0.8455	0.8894	0.1927	0.2161

Table 2. Performance evaluations on DocVQA [21] by Average Normalized Levenshtein Similarity (ANLS) for different methods using LLaVA and InternVL models.

Methods	Bitwidth b	Perception (\uparrow)		Overall (\uparrow)	
		internvl-2.5			
		8b	26b	8b	26b
Baseline	16	1.53	1.68	1.50	1.68
KIVI	8	1.49	1.67	1.47	1.65
VLCache	8	1.53	1.68	1.51	1.67
Ours	8	1.53	1.68	1.50	1.68
KIVI	4	1.50	1.66	1.47	1.65
VLCache	4	1.53	1.68	1.50	1.67
Ours	4	1.54	1.69	1.51	1.68
KIVI	2	1.50	1.64	1.47	1.63
VLCache	2	1.51	1.64	1.49	1.64
Ours	2	1.50	1.67	1.47	1.66
KIVI	1	1.39	1.52	1.31	1.51
VLCache	1	1.50	1.65	1.48	1.64
Ours	1	1.49	1.63	1.45	1.62

Table 3. Performance evaluations on MMBench-Video [11] by perception and overall scores for different methods using InternVL models.

For example, when $n = 3329$ for 8B parameter model, we achieve 126.582 tokens/s at 5 GB (versus 11.628 tokens/s for the baseline) and it scales to 459.016 tokens/s at 30 GB (versus 40.816 tokens/s for the baseline). This represents a throughput boost of approximately $9.88\times$ to $11.24\times$ over the baseline, showing the efficacy of our approach in enhancing decoding performance under constrained memory conditions. We have attached detailed throughput data as an appendix to the paper.

5.5. Ablation Study

We conduct two ablation studies to validate our key contributions: the calibration technique and channel-wise quantization applied to the value cache. We replicate the image

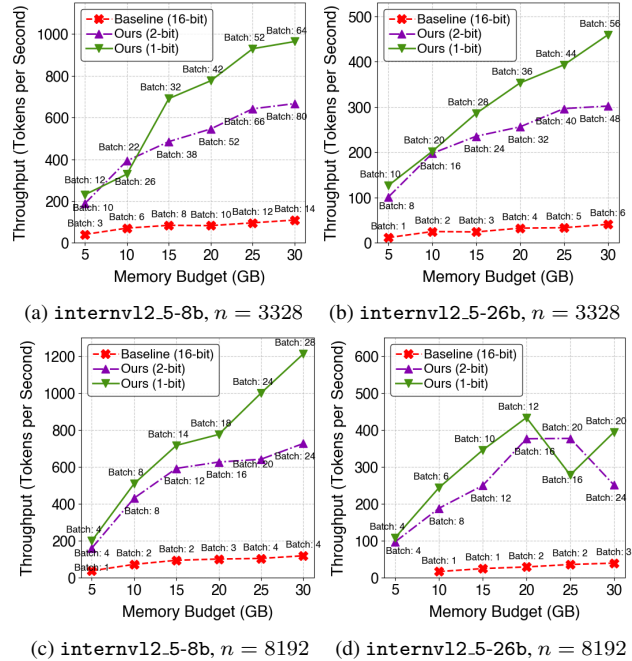


Figure 3. Throughputs of our 2-bit, 1-bit quantization and the baseline (16-bit) across various memory budgets (5 to 30 GB). We use 2 models: `internvl2.5-8b` and `internvl2.5-26b`, and the visual token lengths are $n = 3328$ and 8192 . The annotated texts indicate the maximum batch size accommodated within each memory budget.

captioning task outlined in Sec. 5.1 using `internvl-2.5-8b` model.

Calibration of Post-quantization. In order to investigate the impact of calibration on pre-softmax attention scores discussed in Sec. 4.2, we fix all hyperparameters of quantization with $b = 1$ and compare evaluation metrics of quantizations with and without calibration. As presented Tab. 4, calibration (Quant-C) substantially outperforms the uncalibration (Quant) for all evaluation metrics. This justifies the crucial role of calibration to achieve promising performances.

Channel-wise Quantization on Value Cache. We additionally compare different quantization approaches for the value cache. In particular, we compare channel-wise to the non-channel-wise, which finds the global minimum and maximum values. In Tab. 4, we observe that non-channel-wise quantization performs worse than the channel-wise one. This supports our approach for the value cache.

6. Conclusion

In this paper, we explore the compression of visual caches in multimodal large language models (MLLMs). Unlike prior

Metrics (\uparrow)	Channel-wise + Calibration	Without Calibration	Without Channel-wise
SPICE	0.231	0.230	0.235
BLEU_1	0.792	0.784	0.792
BLEU_2	0.625	0.617	0.609
BLEU_3	0.471	0.464	0.457
BLEU_4	0.346	0.339	0.334
METEOR	0.287	0.285	0.288
ROUGE_L	0.577	0.572	0.571
CIDEr	1.231	1.194	1.200

Table 4. Comparison of calibration on pre-softmax attentions and channel-wise quantization on the value cache on the COCO Caption dataset.

work that focuses on token dropping, we investigate quantization techniques specifically designed for visual tokens, enabling lower-bit representations. A naïve quantization to extreme bit levels often induces distribution shifts, leading to degraded performance. To address this, we propose a novel calibration strategy for pre-softmax attention scores, mitigating quantization-induced distortions. Additionally, we introduce a post-scaling technique for efficient channel-wise cache quantization. Experiments on the InternVL model family for COCO Caption, MMBench-Video, and DocVQA benchmarks demonstrate the effectiveness of our approach.

References

- [1] Marah Abdin, Jyoti Aneja, Hany Awadalla, Ahmed Awadallah, Ammar Ahmad Awan, Nguyen Bach, Amit Bahree, Arash Bakhtiari, Jianmin Bao, Harkirat Behl, et al. Phi-3 technical report: A highly capable language model locally on your phone. *arXiv preprint arXiv:2404.14219*, 2024. 1, 2
- [2] Dzmitry Bahdanau, Kyunghyun Cho, and Yoshua Bengio. Neural machine translation by jointly learning to align and translate. *arXiv preprint arXiv:1409.0473*, 2014. 1
- [3] Jinze Bai, Shuai Bai, Shusheng Yang, Shijie Wang, Sinan Tan, Peng Wang, Junyang Lin, Chang Zhou, and Jingren Zhou. Qwen-vl: A frontier large vision-language model with versatile abilities. *arXiv preprint arXiv:2308.12966*, 2023. 1
- [4] Zefan Cai, Yichi Zhang, Bofei Gao, Yuliang Liu, Tianyu Liu, Keming Lu, Wayne Xiong, Yue Dong, Baobao Chang, Junjie Hu, et al. Pyramidkv: Dynamic kv cache compression based on pyramidal information funneling. *arXiv preprint arXiv:2406.02069*, 2024. 2
- [5] Dongping Chen, Ruoxi Chen, Shilin Zhang, Yinuo Liu, Yaochen Wang, Huichi Zhou, Qihui Zhang, Yao Wan, Pan Zhou, and Lichao Sun. Mllm-as-a-judge: Assessing multi-modal llm-as-a-judge with vision-language benchmark. *arXiv preprint arXiv:2402.04788*, 2024. 1
- [6] Liang Chen, Haozhe Zhao, Tianyu Liu, Shuai Bai, Junyang Lin, Chang Zhou, and Baobao Chang. An image is worth 1/2 tokens after layer 2: Plug-and-play inference acceleration for large vision-language models. In *European Conference on Computer Vision*, pages 19–35. Springer, 2024. 2
- [7] Xinlei Chen, Hao Fang, Tsung-Yi Lin, Ramakrishna Vedantam, Saurabh Gupta, Piotr Dollár, and C Lawrence Zitnick. Microsoft coco captions: Data collection and evaluation server. *arXiv preprint arXiv:1504.00325*, 2015. 4, 5, 7
- [8] Xiangxiang Chu, Limeng Qiao, Xinyang Lin, Shuang Xu, Yang Yang, Yiming Hu, Fei Wei, Xinyu Zhang, Bo Zhang, Xiaolin Wei, et al. Mobilevlm: A fast, strong and open vision language assistant for mobile devices. *arXiv preprint arXiv:2312.16886*, 2023. 2
- [9] Xiangxiang Chu, Limeng Qiao, Xinyu Zhang, Shuang Xu, Fei Wei, Yang Yang, Xiaofei Sun, Yiming Hu, Xinyang Lin, Bo Zhang, et al. Mobilevlm v2: Faster and stronger baseline for vision language model. *arXiv preprint arXiv:2402.03766*, 2024. 2
- [10] Damai Dai, Chengqi Deng, Chenggang Zhao, RX Xu, Huazuo Gao, Deli Chen, Jiashi Li, Wangding Zeng, Xingkai Yu, Y Wu, et al. Deepseekmoe: Towards ultimate expert specialization in mixture-of-experts language models. *arXiv preprint arXiv:2401.06066*, 2024. 1
- [11] Xinyu Fang, Kangrui Mao, Haodong Duan, Xiangyu Zhao, Yining Li, Dahua Lin, and Kai Chen. Mmbench-video: A long-form multi-shot benchmark for holistic video understanding. *arXiv preprint arXiv:2406.14515*, 2024. 5, 6, 8
- [12] Insu Han, Praneeth Kacham, Amin Karbasi, Vahab Mirrokni, and Amir Zandieh. Polarquant: Quantizing kv caches with polar transformation. *arXiv preprint arXiv:2502.02617*, 2025. 1
- [13] Insu Han, Michael Kapralov, Ekaterina Kochetkova, Kshiteej Sheth, and Amir Zandieh. Balancekv: Kv cache compression through discrepancy theory. *arXiv preprint arXiv:2502.07861*, 2025. 1
- [14] Coleman Hooper, Sehoon Kim, Hiva Mohammadzadeh, Michael W Mahoney, Sophia Shao, Kurt Keutzer, and Amir Gholami. Kvquant: Towards 10 million context length llm inference with kv cache quantization. *Advances in Neural Information Processing Systems*, 37:1270–1303, 2024. 2
- [15] Albert Q Jiang, Alexandre Sablayrolles, Antoine Roux, Arthur Mensch, Blanche Savary, Chris Bamford, Devendra Singh Chaplot, Diego de las Casas, Emma Bou Hanna, Florian Bressand, et al. Mixtral of experts. *arXiv preprint arXiv:2401.04088*, 2024. 1
- [16] Hongye Jin, Xiaotian Han, Jingfeng Yang, Zhimeng Jiang, Zirui Liu, Chia-Yuan Chang, Huiyuan Chen, and Xia Hu. Llm maybe longlm: Self-extend llm context window without tuning. *arXiv preprint arXiv:2401.01325*, 2024. 2
- [17] Woosuk Kwon, Zhuohan Li, Siyuan Zhuang, Ying Sheng, Lianmin Zheng, Cody Hao Yu, Joseph Gonzalez, Hao Zhang, and Ion Stoica. Efficient memory management for large language model serving with pagedattention. In *Proceedings of the 29th Symposium on Operating Systems Principles*, pages 611–626, 2023. 2
- [18] Yanwei Li, Yuechen Zhang, Chengyao Wang, Zhisheng Zhong, Yixin Chen, Ruihang Chu, Shaoteng Liu, and Jiaya Jia. Mini-gemini: Mining the potential of multi-modality vision language models. *arXiv preprint arXiv:2403.18814*, 2024. 2
- [19] Bin Lin, Zhenyu Tang, Yang Ye, Jiaxi Cui, Bin Zhu, Peng Jin, Jinfa Huang, Junwu Zhang, Yatian Pang, Munan Ning,

- et al. Moe-llava: Mixture of experts for large vision-language models. *arXiv preprint arXiv:2401.15947*, 2024. 2
- [20] Zirui Liu, Jiayi Yuan, Hongye Jin, Shaochen Zhong, Zhaozhuo Xu, Vladimir Braverman, Beidi Chen, and Xia Hu. Kivi: A tuning-free asymmetric 2bit quantization for kv cache. In *International Conference on Machine Learning*, 2024. 1, 2, 3, 6
- [21] Minesh Mathew, Dimosthenis Karatzas, and CV Jawahar. Docvqa: A dataset for vqa on document images. In *Proceedings of the IEEE/CVF winter conference on applications of computer vision*, pages 2200–2209, 2021. 5, 6, 8
- [22] Bitar Darvish Rouhani, Nitin Garegrat, Tom Savell, Ankit More, Kyung-Nam Han, Ritchie Zhao, Mathew Hall, Jasmine Klar, Eric Chung, Yuan Yu, Michael Schulte, Ralph Wittig, Ian Bratt, Nigel Stephens, Jelena Milanovic, John Brothers, Pradeep Dubey, Marius Cornea, Alexander Heinecke, Andres Rodriguez, Martin Langhammer, Summer Deng, Maxim Naumov, Paulius Micikevicius, Michael Siu, and Colin Verrilli. OCP micro scaling formats mx v1.0 specification. Technical report, Open Compute Project, 2023. Version 1.0. 4
- [23] Yuzhang Shang, Mu Cai, Bingxin Xu, Yong Jae Lee, and Yan Yan. Llava-prumerge: Adaptive token reduction for efficient large multimodal models. *arXiv preprint arXiv:2403.15388*, 2024. 2
- [24] Yunlong Tang, Jing Bi, Siting Xu, Luchuan Song, Susan Liang, Teng Wang, Daoan Zhang, Jie An, Jingyang Lin, Rongyi Zhu, et al. Video understanding with large language models: A survey. *arXiv preprint arXiv:2312.17432*, 2023. 1
- [25] Philippe Tillet, H. T. Kung, and David Cox. Triton: an intermediate language and compiler for tiled neural network computations. In *Proceedings of the 3rd ACM SIGPLAN International Workshop on Machine Learning and Programming Languages*, page 10–19, New York, NY, USA, 2019. Association for Computing Machinery. 5
- [26] Dezhao Tu, Danylo Vashchilenko, Yuzhe Lu, and Panpan Xu. V1-cache: Sparsity and modality-aware kv cache compression for vision-language model inference acceleration. *arXiv preprint arXiv:2410.23317*, 2024. 6
- [27] A Vaswani. Attention is all you need. *Advances in Neural Information Processing Systems*, 2017. 2
- [28] Zhongwei Wan, Ziang Wu, Che Liu, Jinfa Huang, Zhihong Zhu, Peng Jin, Longyue Wang, and Li Yuan. Look-m: Look-once optimization in kv cache for efficient multimodal long-context inference. *arXiv preprint arXiv:2406.18139*, 2024. 1
- [29] Hao Wu, Patrick Judd, Xiaojie Zhang, Mikhail Isaev, and Paulius Micikevicius. Integer quantization for deep learning inference: Principles and empirical evaluation. *arXiv preprint arXiv:2004.09602*, 2020. 1
- [30] Long Xing, Qidong Huang, Xiaoyi Dong, Jiajie Lu, Pan Zhang, Yuhang Zang, Yuhang Cao, Conghui He, Jiaqi Wang, Feng Wu, et al. Pyramiddrop: Accelerating your large vision-language models via pyramid visual redundancy reduction. *arXiv preprint arXiv:2410.17247*, 2024. 2
- [31] Yuan Yao, Tianyu Yu, Ao Zhang, Chongyi Wang, Junbo Cui, Hongji Zhu, Tianchi Cai, Haoyu Li, Weilin Zhao, Zhihui He, et al. Minicpm-v: A gpt-4v level mllm on your phone. *arXiv preprint arXiv:2408.01800*, 2024. 2
- [32] Amir Zandieh, Majid Daliri, and Insu Han. Qjl: 1-bit quantized jl transform for kv cache quantization with zero overhead. *arXiv preprint arXiv:2406.03482*, 2024. 1, 2
- [33] Amir Zandieh, Insu Han, Vahab Mirrokni, and Amin Karbasi. Subgen: Token generation in sublinear time and memory. *arXiv preprint arXiv:2402.06082*, 2024.
- [34] Zhenyu Zhang, Ying Sheng, Tianyi Zhou, Tianlong Chen, Lianmin Zheng, Ruisi Cai, Zhao Song, Yuandong Tian, Christopher Ré, Clark Barrett, et al. H2o: Heavy-hitter oracle for efficient generative inference of large language models. *Advances in Neural Information Processing Systems*, 36:34661–34710, 2023. 1, 2
- [35] Zeliang Zhang, Xiaodong Liu, Hao Cheng, Chenliang Xu, and Jianfeng Gao. Diversifying the expert knowledge for task-agnostic pruning in sparse mixture-of-experts. *arXiv preprint arXiv:2407.09590*, 2024. 1
- [36] Zeliang Zhang, Phu Pham, Wentian Zhao, Kun Wan, Yu-Jhe Li, Jianing Zhou, Daniel Miranda, Ajinkya Kale, and Chenliang Xu. Treat visual tokens as text? but your mllm only needs fewer efforts to see. *arXiv preprint arXiv:2410.06169*, 2024. 1, 2

Appendix

A. Throughput Analysis

We analyzed the throughputs on InternVL models with different token lengths on H100. The results are shown in the following tables. Tab. 5 and Tab. 6 covers the results with sequence length 3328 and parameters $8B$ and $26B$ respectively. Tab. 7 and Tab. 8 covers the results with larger sequence length (8192) and the same parameter configurations.

Model	Memory (GB)	Max BS	Prefill Speed	Decode Speed (s/token)	Throughput Decode	Throughput Overall (500 tokens)
internvl-8b-16bit	5	3	0.117	0.074	40.54	0.0808
	10	6	0.176	0.085	70.59	0.1406
	15	8	0.212	0.095	84.21	0.1677
	20	10	0.253	0.121	82.64	0.1646
	25	12	0.293	0.125	96.00	0.1911
	30	14	0.365	0.128	109.38	0.2175
internvl-8b-ours-1bit	5	12	0.362	0.052	230.77	0.4552
	10	26	0.734	0.079	329.11	0.6462
	15	38	1.046	0.055	690.91	1.3312
	20	52	1.510	0.067	776.12	1.4853
	25	66	1.868	0.071	929.58	1.7662
	30	80	2.225	0.083	963.86	1.8296
internvl-8b-ours-2bit	5	10	0.294	0.053	188.68	0.3732
	10	22	0.623	0.056	392.86	0.7686
	15	32	0.957	0.066	484.85	0.9424
	20	42	1.156	0.077	545.45	1.0591
	25	52	1.515	0.081	641.98	1.2377
	30	64	1.813	0.096	666.67	1.2848

Table 5. Throughput of our method on InternVL-8B model with varying memory budgets on H100 with sequence length 3328

Model	Memory (GB)	Max BS	Prefill Speed	Decode Speed (s/token)	Throughput Decode	Throughput Overall (500 tokens)
internvl-26b-16bit	5	1	0.067	0.086	11.63	0.0232
	10	2	0.116	0.080	25.00	0.0499
	15	3	0.167	0.124	24.19	0.0483
	20	4	0.210	0.123	32.52	0.0648
	25	5	0.275	0.149	33.56	0.0669
	30	6	0.319	0.147	40.82	0.0813
internvl-26b-ours-1bit	5	10	0.703	0.079	126.58	0.2487
	10	20	1.181	0.099	202.02	0.3946
	15	28	1.772	0.098	285.71	0.5515
	20	36	2.246	0.102	352.94	0.6761
	25	44	2.951	0.112	392.86	0.7464
	30	56	3.800	0.122	459.02	0.8642
internvl-26b-ours-2bit	5	8	0.591	0.079	101.27	0.1995
	10	16	1.216	0.081	197.53	0.3835
	15	24	1.553	0.102	235.29	0.4567
	20	32	2.199	0.125	256.00	0.4946
	25	40	2.619	0.135	296.30	0.5705
	30	48	3.051	0.159	301.89	0.5815

Table 6. Throughput of our method on InternVL-26B model with varying memory budgets on H100 with sequence length 3328

A.1. Details for Low-bit Quantization with Packing

Suppose we aim to quantize data into N -bit values and pack them into an M -bit integer, where M must be divisible by N . Along the quantization dimension (which is contiguous in memory), we partition the data into groups of size $\frac{M}{N}$. For each i -th element (starting from 0) within a group v , we left-shift the corresponding quantized value $v[i]$ by $M - N(1 + i)$ bits. The packed integer is obtained by summing these shifted values. Since the shifted bits occupy non-overlapping positions, this summation is equivalent to a bitwise OR operation. Formally, the packing function is defined as:

Model	Memory (GB)	Max BS	Prefill Speed	Decode Speed (s/token)	Throughput Decode	Throughput Overall (500 tokens)
internvl-8b-16bit	5	1	0.115	0.078	38.46	0.0767
	10	2	0.177	0.082	73.17	0.1457
	15	2	0.176	0.084	95.24	0.1897
	20	3	0.236	0.098	102.04	0.2031
	25	4	0.294	0.114	105.26	0.2094
	30	4	0.294	0.117	119.66	0.2381
internvl-8b-ours-1bit	5	4	0.299	0.060	200.00	0.3961
	10	8	0.581	0.051	509.80	0.9969
	15	14	0.941	0.053	716.98	1.3848
	20	18	1.210	0.067	776.12	1.4981
	25	24	1.590	0.066	1000.00	1.9081
	30	28	3.110	0.066	1212.12	2.2155
internvl-8b-ours-2bit	5	4	0.300	0.062	161.29	0.3195
	10	8	0.584	0.051	431.37	0.8434
	15	12	0.813	0.054	592.59	1.1505
	20	16	1.074	0.067	626.87	1.2148
	25	20	1.358	0.081	641.98	1.2423
	30	24	1.598	0.088	727.27	1.4036

Table 7. Throughput of our method on InternVL-8B model with varying memory budgets on H100 with sequence length 8192

Model	Memory (GB)	Max BS	Prefill Speed	Decode Speed (s/token)	Throughput Decode	Throughput Overall (500 tokens)
internvl-26b-16bit	5	1	–	–	–	–
	10	1	0.136	0.117	17.09	0.0341
	15	1	0.136	0.119	25.21	0.0503
	20	2	0.263	0.135	29.63	0.0590
	25	2	0.263	0.138	36.23	0.0722
	30	3	0.381	0.150	40.00	0.0796
internvl-26b-ours-1bit	5	4	0.691	0.092	108.70	0.2142
	10	6	1.069	0.082	243.90	0.4754
	15	10	1.560	0.081	345.68	0.6657
	20	12	1.848	0.083	433.73	0.8305
	25	16	2.540	0.158	278.48	0.5396
	30	20	3.103	0.142	394.37	0.7557
internvl-26b-ours-2bit	5	2	0.358	0.082	97.56	0.1934
	10	4	0.677	0.085	188.24	0.3706
	15	6	0.943	0.096	250.00	0.4904
	20	10	1.574	0.085	376.47	0.7261
	25	12	1.857	0.106	377.36	0.7292
	30	16	2.550	0.191	251.31	0.4895

Table 8. Throughput of our method on InternVL-26B model with varying memory budgets on H100 with sequence length 8192

$$\text{pack}(v, N, M) = v^\top \begin{bmatrix} 2^{M-N} \\ 2^{M-2N} \\ \vdots \\ 2^N \\ 1 \end{bmatrix}$$

Conversely, the unpack operation reverses the packing process and is formally defined as:

$$\text{unpack}(u, N, M) = \left(u \cdot \begin{bmatrix} 2^{N-M} \\ 2^{2N-M} \\ \vdots \\ 2^{-N} \\ 1 \end{bmatrix} \right) \pmod{2^N}$$

Here, the i -th element (starting from 0) is extracted by right-shifting the packed integer u by $M - N(1 + i)$ bits, then applying a modulo 2^N to isolate the N -bit value. The modulo operation is equivalent to a bitwise AND with $2^N - 1$, masking all but the least significant N bits.